Alignment and Deformation for Cryostat of CADS Injector Ⅱ

Jiandong Yuan, Lizhen Ma, Yuan He, Bin Zhang, Juihui Zhang, Guozhen Sun

Presenter: Jiandong Yuan

Institute of Modern Physics, Chinese Acadmey of Science(IMP,CAS)

2018.10

Email:yuanjiandong@impcas.ac.cn

Outline

1 CADS/CiADS Introduction

2 Cryostat in IMP,CAS

3 Alignment methods

4 Simulating Calculation

5 Monitoring Analysis

6 Results Discussion

7 Conclusion

1.1 CADS Introduction

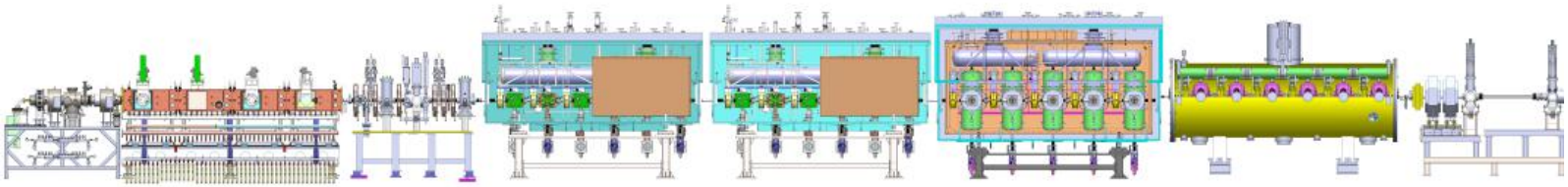

As a front-end demo facility of CiADS, CADS contians ECR Ion source, LEBT, RFQ, MEBT, Cryostat and HEBT.On June 5 to 7, 2017, CADS Injector Ⅱ realized the pulse proton beam energy of 26.1 MeV, pulse current of 12.6 mA. And CADS achieved continuous wave proton beam energy of 25.0 MeV, continuous wave high power proton current of 150~200 uA.

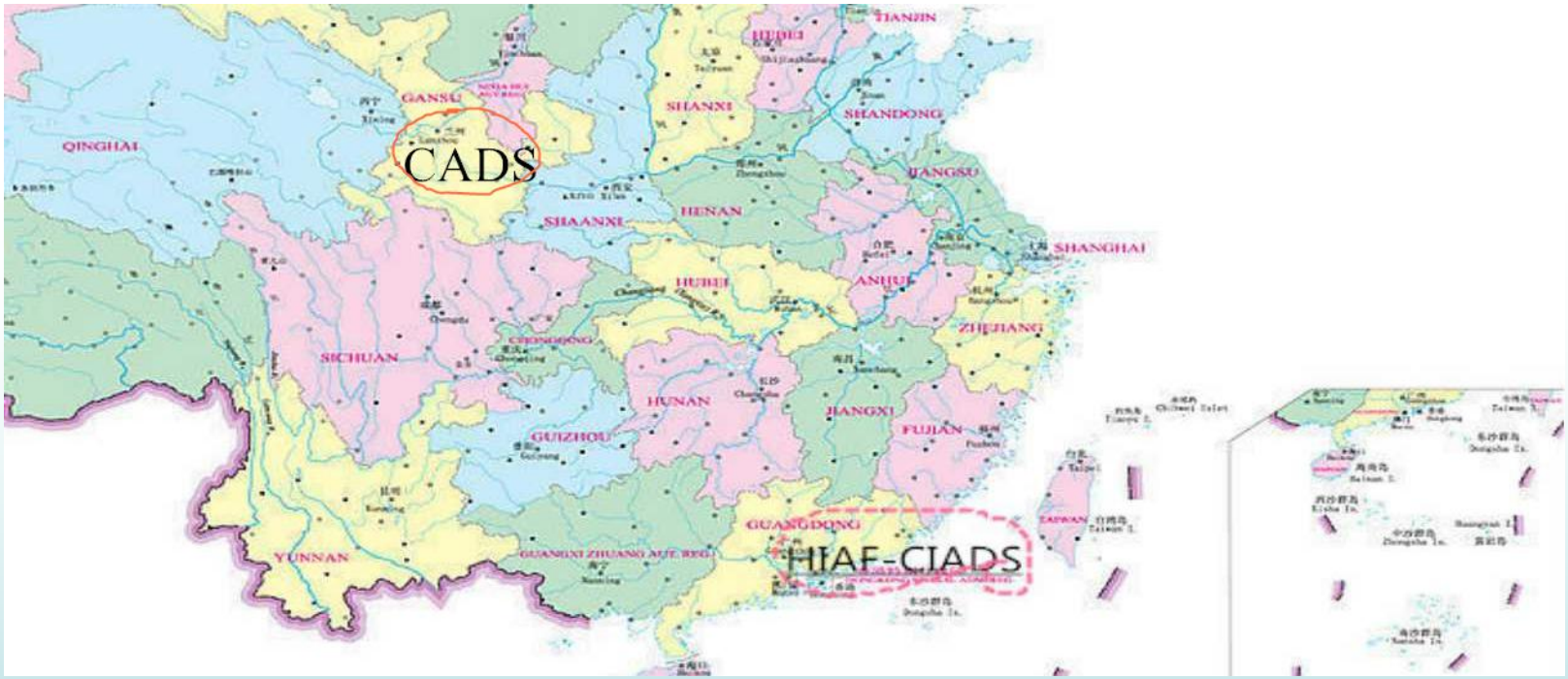

1.2 CiADS Introduction

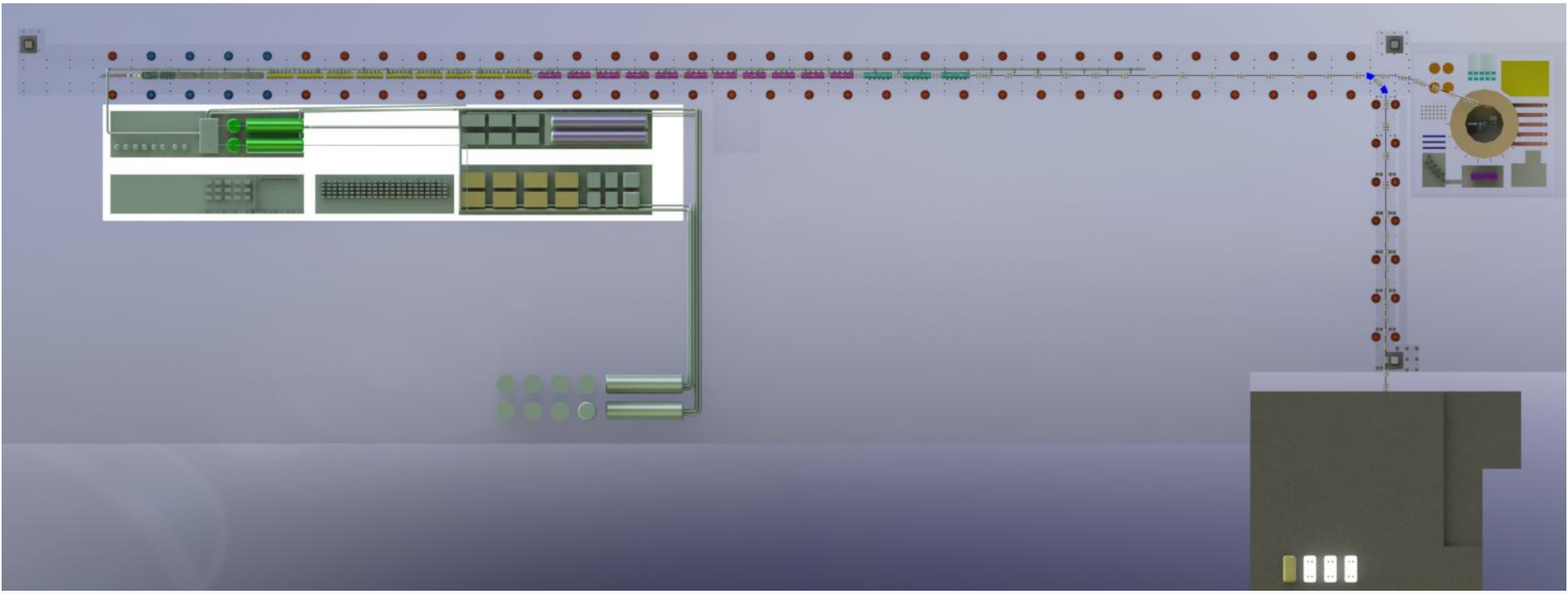

The CiADS accelerator is capable of transmuting radioactive nuclear wastes and meanwhile producing energy in a clean and safe way, aiming to produce a maximum design current of 15 mA at the 1.5 GeV energy with an operating frequency of 162.5 MHz. CiADS consists of 250 quadrupoles, 8 dipoles, 29 cryostats, 4 RFQ, 1 spallation target and 1 subcritical reactor.

2.1 Cryostat in IMP,CAS

1st generation: one cavity

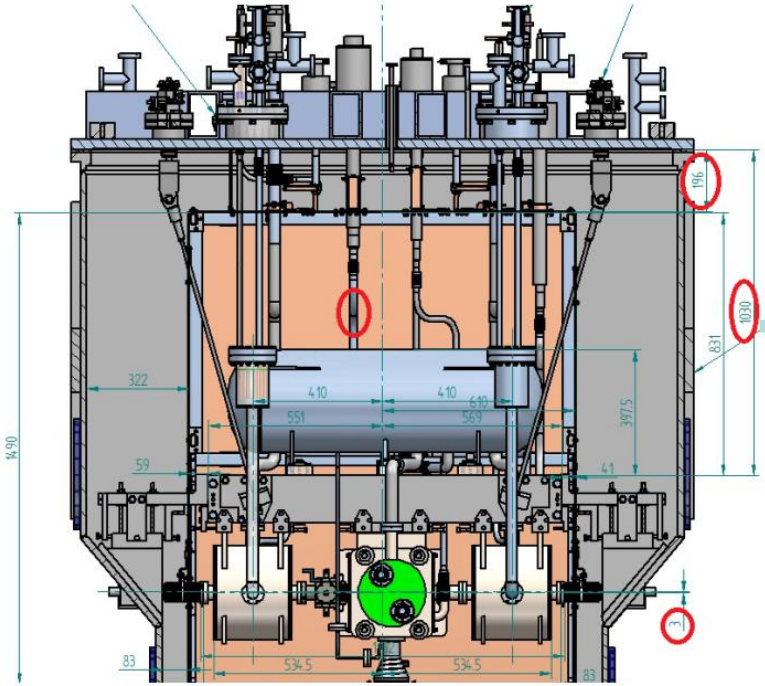

2nd generation: six cavities

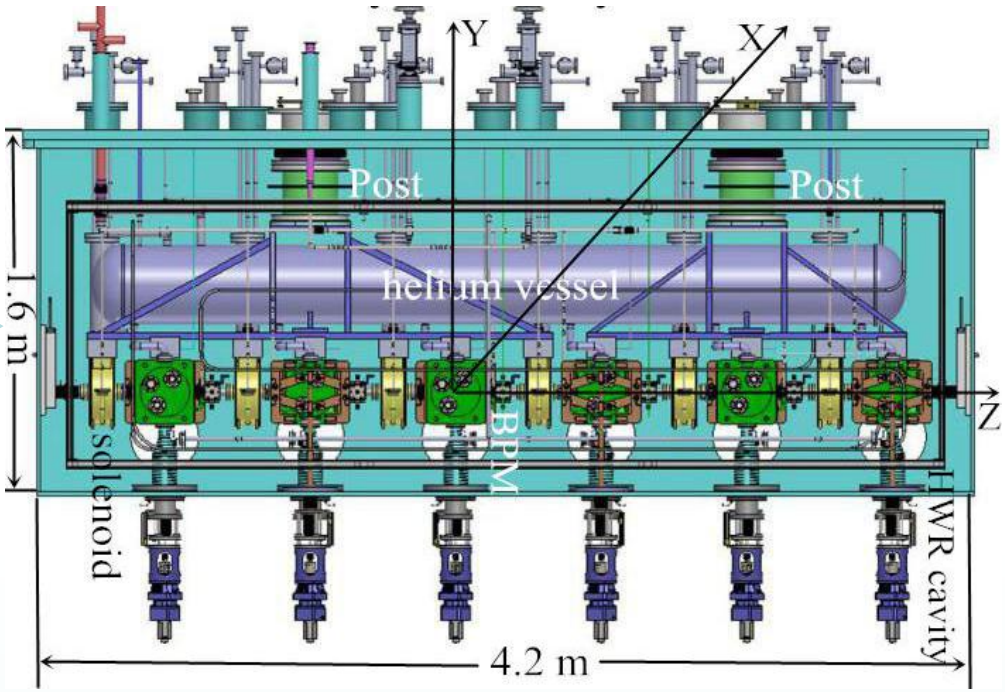

CADS injector Ⅱ project includes four cryostats. The first three cryostats were develpoed by IMP,CAS. The 4th cryostat was developed by IHEP,CAS. Their alignment will be carried out at room temperature first, and then after the contraction, the position error of the cavities and magnets shall be within ±0.5mm.

2.2 Alignment Tolerance in IMP,CAS

Errors	Displacement			Rotation		
	Dx(mm)	Dy(mm)	Dz(mm)	Rx(mrad)	Ry(mrad)	Rz(mrad)
BPM	0.5	0.5	1	2	2	2
Solenoid	0.5	0.5	1	2	2	2
Cavity	1	1	1	2	2	2
CM	1	1	1	5	5	5

Because of the requirements of high reliability and low beam losses, the tolerance of alignment are very strict (4K).

2.3 Alignment Process in IMP,CAS

HWR

Control Network

Single component's calibration

Bundle component's calibration

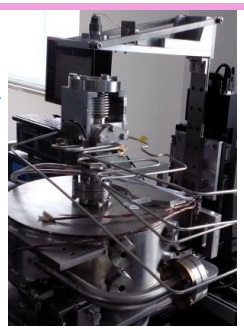

BPM+Solenoid

Offline alignment and monitoring

Online alignment

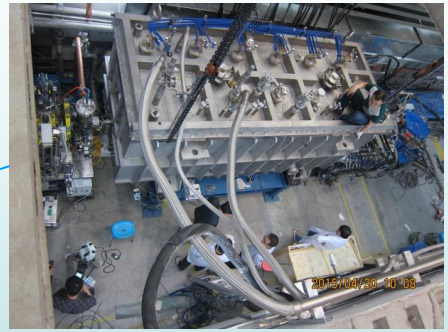

3 Cryostat Alignment Methods

COUNTRIES	LAB	Installment Instruments	Monitoring Device
Germany	DESY	Laser Tracker, Portable CMM	Wire Position Monitor
	GSI	Laser Tracker?	Laser Tracker
USA	SLAC	Micro Alignment Telescope,Laser Tracker	Wire Position Monitor
	Fermi	Theodolite,Laser Tracker	Wire Position Monitor
	MSU	Portable CMM,Laser Tracker	Wire Position Monitor
	Argonne	Theodolite,Laser Tracker	Micro Alignment Telescope, Cryoscanner?
	Jefferson	Theodolite,Level,Laser Tracker, Portable CMM	Micro Alignment Telescope
	SNS	Theodolite...	Micro Alignment Telescope
ITALY	INFN	Laser Tracker, Total Station	Wire Position Monitor
	ELETTRA	Laser Tracker, Portable CMM	Wire Position Monitor
JAPAN	KEK	Laser Tracker, Level, Theodolite,Portable CMM	White Light Interferometer Wire Position Monitor
FRANCE	SPIRAL2	Laser Tracker, Total Station	Micro Alignment Telescope
	CERN	Laser Tracker, Total Station	Brandeis CCD Angle Monitor
CANADA	TRIUMF	Laser Tracker, Portable CMM	Wire Position Monitor
CHINA	IHEP	Laser Tracker	Wire Position Monitor Theodolite+Level
	IMP	Laser Tracker	Micro Alignment Telescope

4.1Simulating

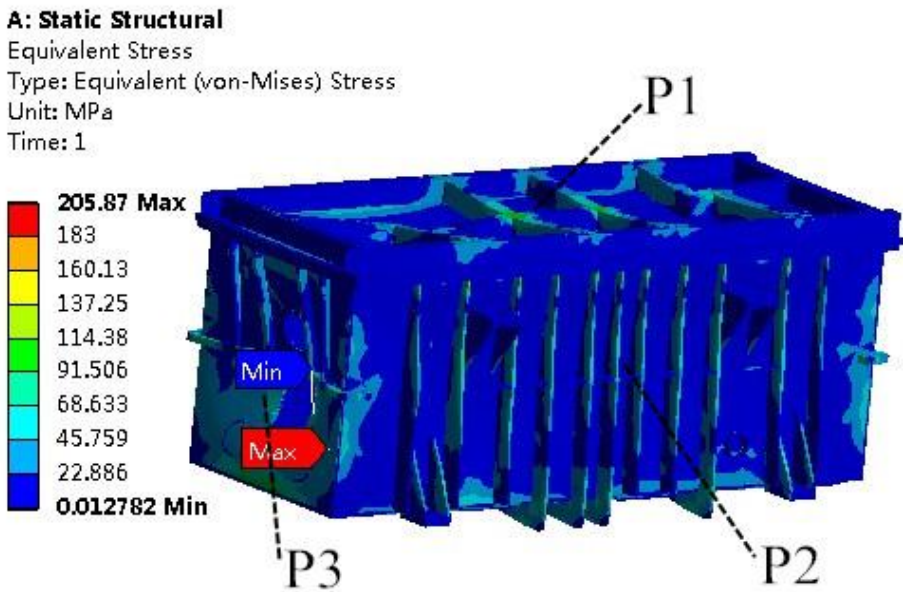

Fig. 2 Stress Simulation (Color online)

The max stress (205.9 MPa) is located at the position of the organic glass. The peak stress value is 183 MPa appears in the two reinforcing bars of the connected stiffeners.The equivalent stress of the main vacuum vessel without organic glass is lower than the allowable stress of the corresponding materials (198 MPa of 316 L stainless steel).

Tab. 1 The boundary conditions, loads and their acting position of the vacuum deformation

NO	Boundary Conditions and Loads	Acting Position
1	The four bottom supports were fixed	Four bottom supports
2	Integral Gravity (1.5 tons, 750 kg per post)	The center of the two posts (G10)
3	Atmospheric Pressure (101.3 KPa)	The six external surface of the vacuum chamber

Vacuum Deformation Simulation

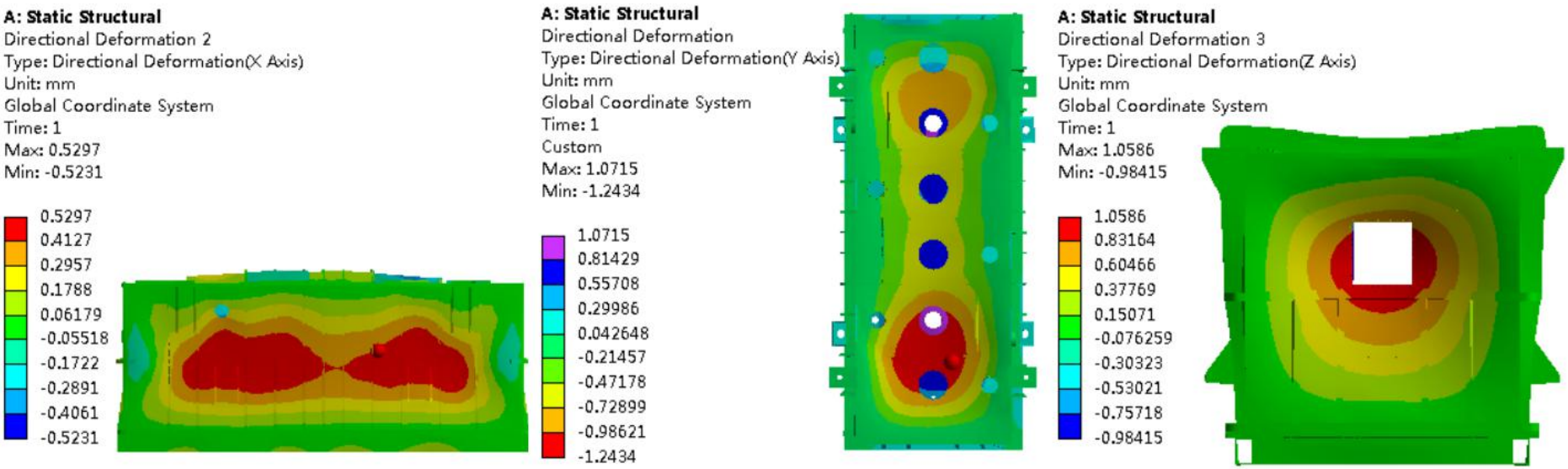

Fig. 3 Vacuum Deformation Simulation (Color online)

The vacuum deformation occurs mainly in the central area around the horizontal vertical and longitudinal zone of vacuum chamber were 0.53, 1.24 and 1.06 mmrespectively. Furthermore the central region is larger than the lateral area. In the horizontal and longitudinal direction, the deformation of the side plate presents an obvious symmetry and equivalence. While in the vertical direction, the max deformation (1.24 mm) occurs in the bottom of the vacuum chamber on account of the lacking of the reinforced stiffeners. However, the max deformation of the top cover plate (1.06 mm) appears mainly in the center of the two posts.

4.2 Cryo-Simulation

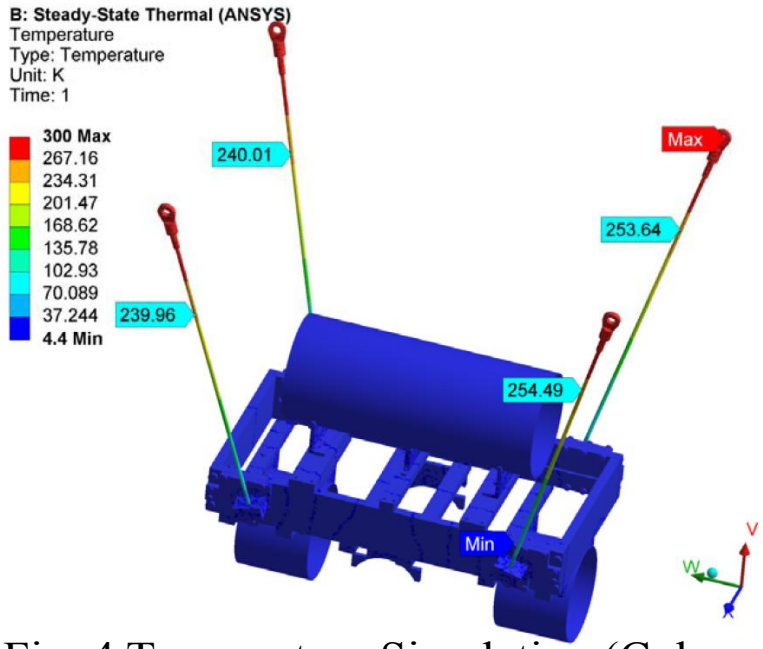

Fig. 4 Temperature Simulation (Color online)

As shown in Tab. 2, the boundary conditions and load [28] contain a self-gravity of the cold mass assembly, a distributive load of temperature, a force of the cold mass assemblies and the top suspending rods.

Tab. 2 The boundary conditions, loads and their acting position of the cryo-deformation

NO	Boundary Conditions and Loads	Acting Position
1	The four rods were fixed	Four top suspending rods
2	Integral Self-Gravity (1.5 tons, 750 kg per post)	The center of the posts (G10)
3	Cold mass Temperature (4K)	The center of the cold mass
4	Rods Temperature (295K)	Four top suspending rods

Simulating Cryo-Deformation

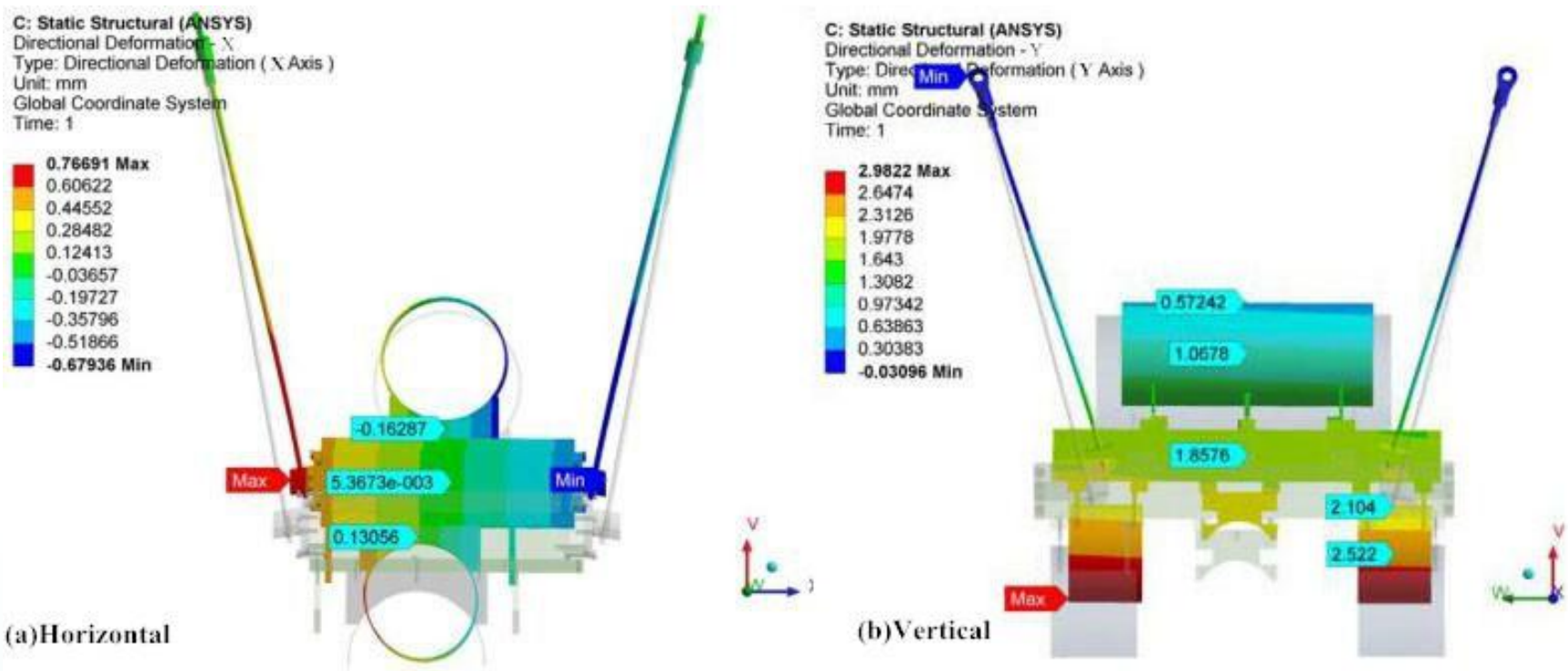

Fig. 5 Cryo-Simulation (Color online)

According to the mechanical characteristics of cold mass and the simulated results(above pictures), the solenoid and HWR cavity were contracted 0.8mm in Horizontal and risen 2.98 mm in Vertical direction，respectively.

5.1 Vacuum Deformation Monitoring

The monitored vacuum deformations are central 0.66 mm in the horizontal direction, 1.32 mm in vertical direction and 0.89 mm in longitudinal direction.

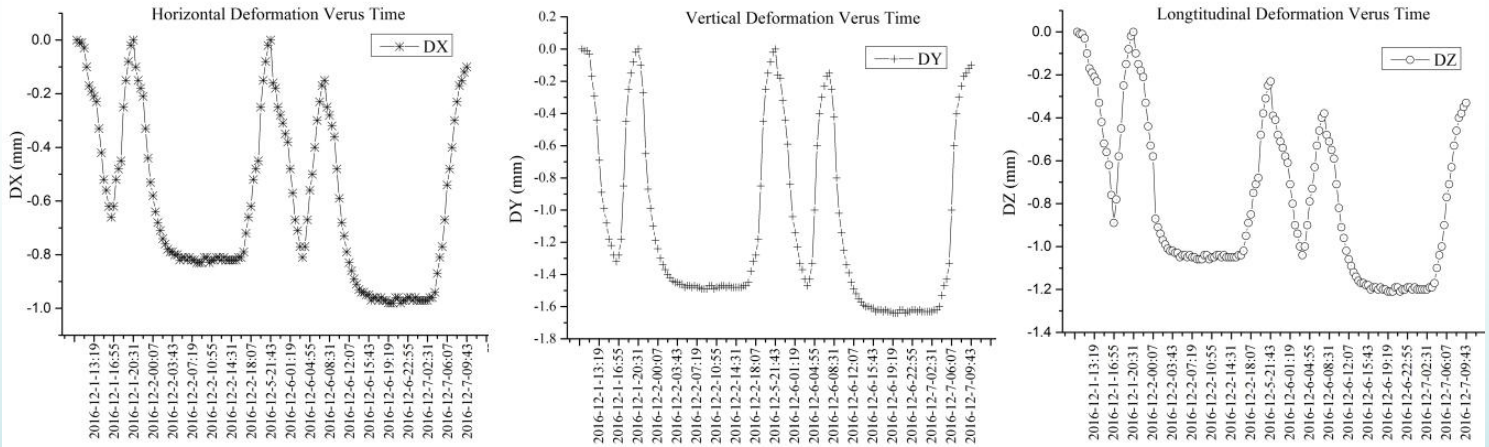

Fig. 6 vacuum deformation monitoring (DX: horizontal; DY: vertical; DZ: longitudinal)

5.2 Cryo-deformation Monitoring

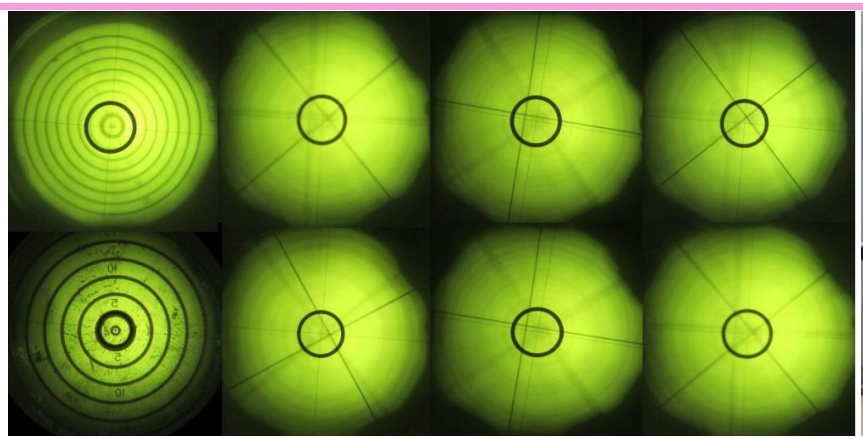

The cold mass was contracted 0.8 mm in horizontal and 2.87 mm in vertical direction.

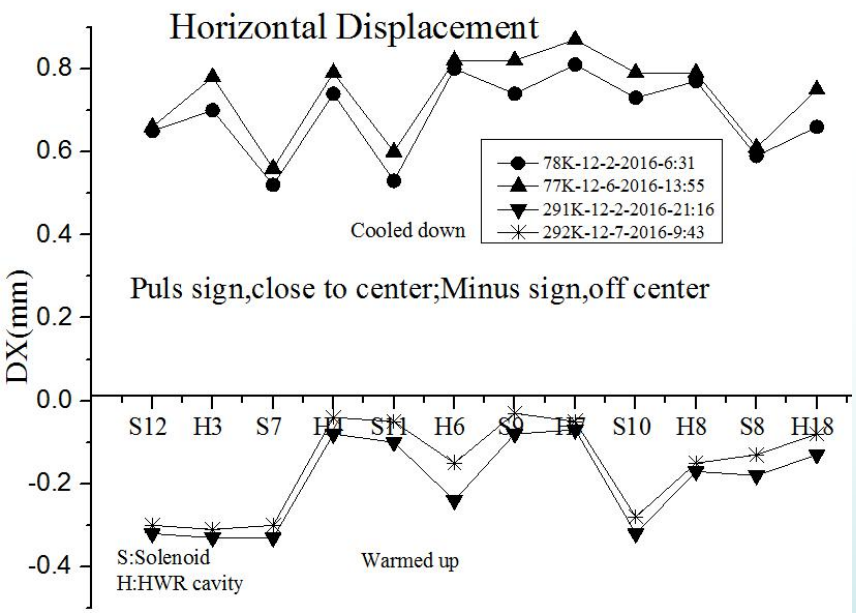

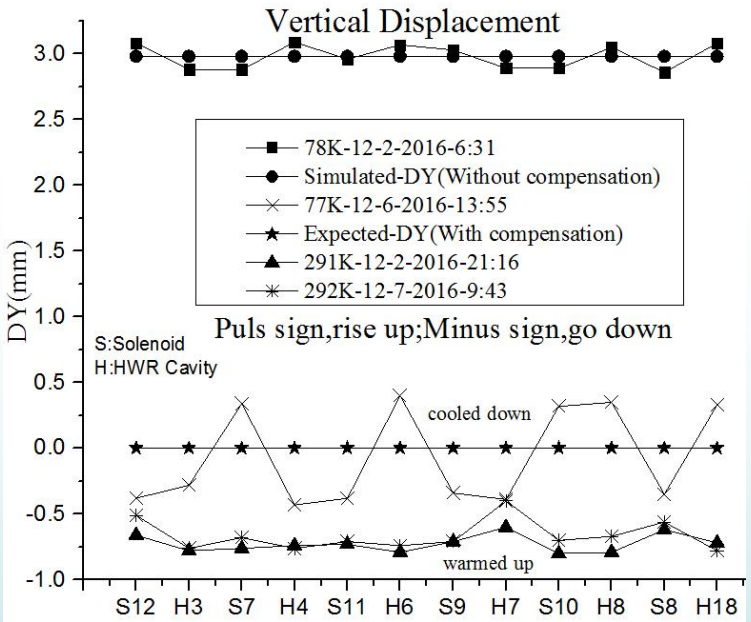

Fig. 7 Cryo-deformation monitoring

6 Discussions

Tab. 3 Results Comparison between simulating and monitoring

Deformation		Simulated	Monitored	Differences
Vacuum	DX (mm)	0.53	0.66	0.13
	DY (mm)	1.24	1.32	0.08
	DZ (mm)	1.06	0.89	0.17
Low temperature	DX (mm)	0.77	0.8	0.03
	DY (mm)	2.98	2.87	0.11

As shown in Tab. 3, the differences of vacuum deformation between simulated and monitored are 0.13 mm in the horizontal direction, 0.08 mm in the vertical direction and 0.17 mm in the vertical direction, respectively;

The differences of cryo-deformation between simulated and monitored are 0.03 mm in horizontal and 0.11 mm in vertical direction on average, respectively.

7 Conclusions

1. The simulated vacuum and cryo-deformation shows a good agreement with the measured values.
2. The cryo-deformation is strongly linked with the vacuum negative pressure, temperature field and the structure of the cryostat.
3. The aligned accuracy fulfilled the requirements and the aligned results guaranteed the success of cw protons.

References

[1] Jijiu Zhao, Yin Zhao Sheng. Particle Accelerator Technology [M]. Beijing: Higher Education Press,2006:30-36(in Chinese).

[2] Zhihui Li, Peng Cheng, Huiping Geng, et al. Physics design of an accelerator for an accelerator-driven subcritical system [J]. PHYSICAL REVIEW SPECIAL TOPICSACCELERATORS AND BEAMS. 2013, 16, 080101-1:080101-23

[3] Shuhui Liu, Zhijun Wang, Huan Jia, et al. Physics design of the CIADS 25 MeV demo facility [J].Nuclear Instruments and Methods in Physics Research A.2017, 843:11-17

[4] Zhijui Wang, Chi Feng, Yuan He, et al. No interceptive transverse emittance measurements using BPM for Chinese ADS R&DProject [J].Nuclear Instruments and Methods in Physics Research A.2016, 816:171-175

[5] Weisend II, J. G. Cryostat Design [M].Springer; 1st ed. 2016 edition (August 13, 2016)

[6] G. Kautzmann, J-C. Gayde, F. Klumb,et al. HIE ISOLDE–GENERAL PRESENTATION OF MATHILDE [C]. The 13th International Workshop on Accelerator Alignment, 13-17 October 2014, IHEP, Beijing, P.R. China.

[7] Hiroshi Sakai, Kazuhiro Enami, Takaaki Furuya, et al. IMPROVEMENT OF THE POSITION MONITOR USING WHITE LIGHT INTERFEROMETER FOR MEASURING PRECISE MOVEMENT OF COMPACT ERL SUPERCONDUCTING CAVITIES IN Cryo module[C].The Proceedings of IPAC2014,Dresden,Germany,2014，TUPRI092:1787-1789.,

[8]A Bertolini. Vibration diagnostics instrumentation for ILC [J].Measurement Science & Technology -MEAS SCI TECHNOL, 2007, 18, 8: 2293-2298

[9] Hongyan Zhu, Lan Dong, Lingling Men, et al. Alignment of ADS beta cryostat with wire position monitors [J]. NUCLEAR SCIENCE AND TECHNIQUES, 2015, 26, 040401:1-4

[10] N. Eddy, B. Fellenz, P. Prieto, et al. A WIRE POSITION MONITOR SYSTEM FOR THE 1.3 GHZ TESLA-STYLE Cryostat AT THE FERMILAB NEW-MUON-LAB ACCELERATOR[C].The 15th International Conference on RF Superconductivity (SRF2011), Chicago, Illinois, USA, 25-29 Jul 2011, 2011, FERMILAB-CONF-11-382-AD.

[11] Remy BEUNARD, Alexis LEFEVRE, François LEGRUEL, SURVEY AND ALIGNMENT CONCEPT FOR THE SPIRAL2 ACCELERATOR (STATUS REPORT) [C].The 11th International Workshop on Accelerator Alignment, DESY, Hamburg, German, September 13-17, (2010)

[12] D. Passarelli, M. Parise, T. H. Nicol, et al. HIGH-VACUUM SIMULATIONS AND MEASUREMENTS ON THE SSR1Cryo module BEAM-LINE[C].Proceedings of SRF2015, Whistler, BC, Canada, TUPB074:754-756

[13] Xiao Long Guo, Li Wang, Jin Wang, et al. Thermal and Mechanical Analysis on the Cold Mass Support Assembly of Test Cryostat for IMP ADS Injector-II [J]. Advances in Cryogenic Engineering, AIP Conf. Proc. 1573, 1341-1348 (2014);
DOI: 10.1063/1.4860862

[14] Frank Marhauser and Kai Tian. Optimization of the Cryo module Cold-to-Warm Transitions and the VTA QA Test Configuration for CEBAF Upgrade Cavities with Regard to Critical HOMs above Cutoff [C].2009, JLAB-TN-09-61

[15] T Powers,T Allison,G Davis, et al. Upgrade to Cryo module Test Facility at Jefferson Lab[J].Accelerators, 2003

[16]Vittorio Parma. Cryostat Design [R].CERN Yellow Report (Accelerator Physics: Instrumentation and Detectors) CERN-2014-005, pp.353-399 DOI:10.5170/CERN-2014-005.353

References

[17] Li Wang, Sen Sun, Shuhua Wang, *et al*. design report of single test cryostat and control valve box in low temperature [R]

[18] J. R. Delayen, L.R. Doolittle, T. Hiatt, *et al.*AN R.F. INPUT COUPLER SYSTEM FOR THE CEBAF ENERGY UPGRADE Cryomodule [C]. Proceedings of the 1999 Particle Accelerator Conference, New York, 1999, 1462-1464

[19] Ruixiong Han, Lin Bian, Rui Ge, *et al*. Development of Vacuum Barrier in 2 K Transfer Lines for Accelerator-Driven Sub-Critical Reactor System [J].CHINESE JOURNAL OF VACUUM SCIENCE AND TECHNOLOGY, 2013, 33(11):1061-1064(In Chinese).

[20] Qingjin Xu, Ohuchi Norihito, Kiyosumi Tsuchiya, *et al.* Thermal simulation and analysis of the STF Cryostat[J].Chinese Physics C.2009, 33(3): 236-239

[21] Carlo Pagani and Paolo Pierini. Cryo module DESIGN, ASSEMBLY AND ALIGNMENT[C]. Proceedings of the 12th International Workshop on RF Superconductivity, Cornell University, Ithaca, New York, USA, SUP04:78-85

[22] A. Saini, V. Lebedev, N.Solyak, *et al.* ESTIMATION OF CRYOGENIC HEAT LOADS IN Cryostat DUE TO THERMAL RADIATION[C]. Proceedings of IPAC2015, Richmond, VA, USA, WEPTY031:3338-3341

[23] Mubeezi, J., Finite Element Analysis (FEA) method, and its Application in Evaluating Stress-Strain Characteristics, Rensselaer at Hartford Engineering Seminar, 2004.

[24] T. S. Datta, Soumen Kar, Jacob Chacko, *et al.* Theoretical analysis for the transient behavior of radiative cooling of cavities in superconducting LINAC cryo module [J]. Heat Mass Transfer (2014) 50:827–833 DOI 10.1007/s00231-013-1281-1

[25] P. J. Barr, M.ASCE1,J. F. Stanton, *et al.* Effects of Temperature Variations on Precast, Prestressed Concrete Bridge Girders [J].JOURNAL OF BRIDGE ENGINEERING.2005, 10, 2:186-194 DOI: 10.1061/ (ASCE) 1084-0702(2005)10:2(186)

[26] Guicheng Du, Xin Ning, Yu Liu. Architectural Mechanics [M]. Dongbei University Publishing House, 2014

[27] Yu Qin Wan, Xiao Fei Niu, Yan Ning Han, *et al.* Cryostat design of ADS Injector [J]. Cryogenics and superconductivity, 2013, 41(12): 25-27

[28] Rui Ge, Ruixiong Han, Lin Bian, *et al.* Design of horizontal test cryostat for Spoke type SRF cavity [J]. CRYOGENICS, 2014, 3:7-10

[29] Jiandong Yuan, Yuan He, Bin Zhang. *et al*. Alignment of beam position monitors in cryomodule of CADS injector Ⅱ[J]. NUCL SCI TECH, (2017) 28: 75. https://doi.org/10.1007/s41365-017-0232-9

[30] A Bertolini, C Pagani, G Varisco. On line monitoring of the TTF Cryostat Cold Mass with Wire Position Monitors. 2000, Marzo, 17, INFN/TC-00/02

[31] N. V. Isaev, T. V. Grigorova, O. V. Mendiuk, *et al.* Plastic deformation mechanisms of ultrafine-grained copper in the temperature range of 4.2–300 K [J].LOW TEMPERATURE PHYSICS, 2016, 42, 9:825-835

[32] http://www.impcas.ac.cn/kyjz2017/201706/t20170622_4816973.html

[33] http://www.impcas.ac.cn/kyjz2017/201706/t20170622_4816980.html

[34]Jiandong Yuan.et al.Deformation Mechanism of the Cryostat in the CADS Injector Ⅱ[J]. Cryogenics 2018(89):113-118

[35]Jiandong Yuan.et al.Simulation Monitoring and Analysis for The Deformation of Cryomodule[J].Vacuum and Cryogenics2018,24(3):182-187


That is all!
Thank you for your kind attention!
图片来源：视觉中国 www.vcg.com

Stress Analysis of Suspension Structure

First and foremost, suspension structure is the simplest but not the best structure for cryostat especially when the cryostat has stringent alignment requirements[5]. Furthermore, the facility for rare isotope beams of michigan state university has proven that the alignment of the bottom-up structure is more efficient than the suspend structure of cryostat[34-35]. Last but not least, since the bottom of the internal cooling mass has no direct contact with the external vacuum chamber of the suspend style cryostat, the cooling mass supported only by one force coming from the post in the vertical direction[36-37]. To sum up, we believe that the bottom-up structure is more stable than the suspend structure for cryostat.

Cryostat Stress Analysis of Suspension Structure